

Published in final edited form as:

*Environ Sci Technol.* 2011 November 1; 45(21): 9232–9239. doi:10.1021/es201702q.

## Environmentally Persistent Free Radicals (EPFRs) - 2. Are Free Hydroxyl Radicals Generated in Aqueous Solutions?

Lavrent Khachatryan and Barry Dellinger

Louisiana State University, Department of Chemistry, Baton Rouge, LA 70803

### Abstract

A chemical spin trap, 5,5-dimethyl-1-pyrroline-N-oxide (DMPO), in conjunction with electron paramagnetic resonance (EPR) spectroscopy was employed to measure the production of hydroxyl radical ( $\cdot\text{OH}$ ) in aqueous suspensions of 5% Cu(II)O/silica (3.9% Cu) particles containing environmentally persistent free radicals (EPFRs) of 2-monochlorophenol (2-MCP). The results indicate: 1) a significant differences in accumulated DMPO-OH adducts between EPFR containing particles and non-EPFR control samples, 2) a strong correlation between the concentration of DMPO-OH adducts and EPFRs per gram of particles, and 3) a slow, constant growth of DMPO-OH concentration over a period of days in solution containing 50  $\mu\text{g}/\text{ml}$  EPFRs particles + DMPO (150 mM) + reagent balanced by 200  $\mu\text{l}$  phosphate buffered (pH = 7.4) saline. However, failure to form secondary radicals using standard scavengers, such as ethanol, dimethylsulfoxide, sodium formate, and sodium azide, suggests *free* hydroxyl radicals may not have been generated in solution. This suggests surface-bound, rather than free, hydroxyl radicals were generated by a surface catalyzed-redox cycle involving both the EPFRs and Cu(II)O. Toxicological studies clearly indicate these bound free radicals promote various types of cardiovascular and pulmonary disease normally attributed to unbound free radicals; however, the exact chemical mechanism deserves further study in light of the implication of formation of bound, rather than free, hydroxyl radicals.

### Keywords

Spin trapping; fine particles; combustion; thermal treatment; biological activity; redox cycling; reactive oxygen species (ROS)

### Introduction

Stable and relatively nonreactive “environmentally persistent free radicals (EPFRs)” have been recently demonstrated to form in the post-flame and cool-zone regions of combustion systems and other thermal processes<sup>1-3</sup>. These resonance-stabilized radicals, including semiquinones, phenoxy, and cyclopentadienyls, can be formed by the thermal decomposition of molecular precursors including catechols, hydroquinones and phenols. Association with the surfaces of fine particles imparts additional stabilization to these radicals such that they can persist almost indefinitely in the environment<sup>2, 4</sup>. A mechanism of chemisorption and electron transfer from the molecular adsorbate to a redox-active transition metal or other receptor is shown through experiment, and supported by molecular

Correspondence to: Barry Dellinger.

Supporting Information **Available**: Details of “Dependence of DMPO-OH adduct generation on biological reducing equivalents”, NADPH and Ascorbic acid, Figures S1 and S2.

This information is available free of charge via the Internet at <http://pubs.acs.org>

orbital calculations, to result in EPFR formation<sup>2, 3, 5</sup>. Both oxygen-centered and carbon-centered EPFRs are possible, the exact structure of which can significantly affect their environmental and biological activity<sup>6, 7</sup>.

An important question is whether EPFRs associated with transition metal oxide-containing nanoparticles can red-ox cycle to generate reactive oxygen species (ROS) such as hydroxyl radicals ( $\cdot\text{OH}$ ), superoxide anion-radicals ( $\text{O}_2^{\cdot-}$ ), and hydrogen peroxide ( $\text{H}_2\text{O}_2$ ) in aqueous media? Information about formation and identification of these ROS has been reported recently<sup>8</sup>. A chemical spin trap 5,5-dimethyl-1-pyrroline-N-oxide (DMPO) in conjunction with electron paramagnetic resonance (EPR) spectroscopy was employed to measure the production of ROS in aqueous suspension of laboratory surrogates of particle-associated EPFRs derived from 2-monochlorophenol (2-MCP) by chemisorption on Cu(II)O/silica particles. The concentration of hydroxyl radicals was measured at  $\sim 1 \mu\text{M}$  for a 140 minute incubation of EPFR-containing solution<sup>8</sup>.

Hydroxyl radical is one of the most aggressive intermediate species responsible for critical tissue damage and oxidative stress<sup>9-12</sup>. However, its high reactivity, and short lifetime may result it in not being able to reach some biological targets. Furthermore, its short half life, makes direct detection of hydroxyl radical virtually impossible; therefore, indirect detection methods such as EPR, coupled with appropriate spin-trapping agents such as 5,5-dimethyl-1-pyrroline-N-oxide (DMPO), has been used<sup>13-17</sup>.

We provide here evidence of *in vitro* generation of hydroxyl radical by EPFRs produced from adsorption of 2-monochlorophenol at 230 °C (2-MCP-230) on copper oxide catalyst supported by silica nanoparticles, 5% Cu(II)O/silica (3.9% Cu)<sup>3, 18</sup>. Our results suggest hydroxyl radicals generated at the interface of the particle and solution remain associated with the surface of the particle.

## Experimental

### Materials

High purity 5,5-dimethyl-1-pyrroline-N-oxide (DMPO, 99 %+, GLC) was obtained from ENZO Life Sciences International and used without further purification. Desferrioxamine, (DFO, assay 92.5%+, TLS); diethylenetriaminepentacetic acid, (DETAPAC, 99%+); L-Ascorbic acid (99%+);  $\beta$ -Nicotinamide Adenine Dinucleotide phosphate, (NADPH, assay,  $\geq 95\%$ ); sodium formate (BioUltra,  $\geq 99\%$ ); sodium azide (BioXtra); dimethyl sulfoxide, (DMSO, 99.7%+); 2-monochlorophenol, (2-MCP, 99%+); copper nitrate hemipentahydrate (99.9%+), 0.01M phosphate buffered saline, (PBS; NaCl 0.138M: KCl 0.0027M), were all obtained from Sigma-Aldrich. Hydrogen peroxide and Cab-O-Sil, as silica powder, were obtained from Fluka (assay, 30%) and Cabot (EH-5, 99%), respectively.

### EPFR surrogate synthesis

5 % CuO/silica (3.9 % Cu), particles were prepared by impregnation of Cab-O-Sil powder with 0.1 M solution of copper nitrate hemipentahydrate and calcinated at 450 °C for 12 h<sup>19</sup>. The sample was then ground and sieved (mesh size 230, 63  $\mu\text{m}$ ). Prior to exposure, the particles were heated in situ in air to 450 °C for 1h to pre-treat the surface. They were then exposed to saturated vapors of 2-MCP at 230 °C using a custom-made vacuum exposure chamber for 5 min. Once exposure was completed, the temperature of the system was cooled to 150 °C for 1 h at  $10^{-2}$  Torr. The EPR spectra were then acquired at ambient conditions to confirm the existence of EPFRs.

## EPR Measurements

EPR spectra were recorded using a Bruker EMX-20/2.7 EPR spectrometer (X-band) with dual cavities, modulation and microwave frequencies 100 kHz and 9.516 GHz, respectively. Typical parameters were: sweep width of 100 G, EPR microwave power of 10 mW, modulation amplitude of 0.8 G, time constant of 40.96 ms, and sweep time of 167.77s. Values of the g-tensor were calculated using Bruker's WIN-EPR SimFonia 2.3 program, which allows control of the Bruker EPR spectrometer, data-acquisition, automation routines, tuning, and calibration programs on a Windows-based PC<sup>20</sup>. The exact g-values for key spectra were determined by comparison with 2, 2-diphenyl-1-picrylhydrazyl (DPPH) standard.

## ROS Generation Studies

Both control and sample solution suspensions, containing particles without EPFRs (CuO/Silica) and with EPFRs (EPFR/CuO/Silica), respectively, were prepared in similar manners. 1 mg/ml suspensions of the control, CuO/silica, and sample, EPFR/CuO/silica, were prepared in water and saturated with air by bubbling for 5 min. Prior to adding DMPO, the surrogate solutions were sonicated 5 min (Fisher Scientific, FS-20) at 40 W. 0.01M PBS was used to maintain the pH at 7.4 and balance the final volume at 200  $\mu$ l. The order of introduction of final solution components to PBS was: particle suspension (10  $\mu$ l from solution of 1 mg/ml), DMPO (10 $\mu$ l from a freshly prepared solution of 3 M), reagents (chelators, ascorbic acid, NADPH), and PBS to balance at 200  $\mu$ l. The final composition of the suspension in most experiments was particles (50  $\mu$ g/ml), DMPO (150 mM), reagent (200  $\mu$ l).

The solutions were stored in the dark and shaken in touch mode for 30 s using a Vortex Genie 2 (Scientific Industries). 20  $\mu$ l of solution was transferred to an EPR capillary tube (i.d.  $\sim$  1 mm, o.d. 1.55mm) and sealed at one end with sealant (Fisherbrand). The capillary was inserted in a 4 mm EPR tube and placed into the EPR resonator<sup>21</sup>. The intensities of the EPR spectra of DMPO-OH adducts were reported in arbitrary units, DI/N, (double integrated (DI) intensity of the EPR spectrum normalized (N) to account for the conversion time, receiver gain, number of data points and sweep width<sup>20</sup>). Each experiment was performed at least twice, and the reported EPR intensities are an average of all spectra obtained for each experiment.

Since the interaction chemistry of chelators with the surface of the model particles is unclear, we abstained from the use of chelators such as DFO, DETAPAC, which minimize the iron content in solution. Chelators have been reported to change drastically the reactivity of particles by affecting the redox potential of metals<sup>22</sup>. Adsorbed EPFRs may also undergo enhanced extraction in the presence of metal chelators, based on the metal-chelate complex stability. The oxidizing species formed by the Fenton-type reactions can also depend on the nature of the iron chelator<sup>23-25</sup>. Non-use of chelators in this work was also based on the fact that the buffer, prepared in deionized water and treated with Chelex 100 ion-exchange resin (Bio-Rad Laboratories, Hercules, LA) to remove trace heavy metal contaminants<sup>26</sup>, did not significantly impact the spin trapping results.

## Results and Discussion

Our model of formation of EPFRs, reduced metals, and ROS via chemisorption of molecular precursors on metal centers is summarized in Scheme 1<sup>8</sup>. The EPFRs formed from 2-MCP adsorbed on CuO/Silica are o-semiquinone (2-hydroxyphenoxy) and 2-chlorophenoxy (latter not shown for clarity)<sup>3</sup>. These EPFRs may red-ox cycle to generate ROS as depicted<sup>8</sup>. The average concentration of EPFRs on Cu(II)O/silica was  $\sim 10^{17}$  spins/g and

exhibited a singlet, structureless EPR spectrum ( $g=2.0042$ ,  $\Delta H_{p-p} = 6.5$  G). Undosed Cu(II)O/silica particles, which did not contain EPFRs, were used as controls. To establish the optimal conditions for generating DMPO-OH adducts, a series of experiments were initially performed in different solvent solutions (water, dimethylsulfoxide (DMSO), and ethanol (EtOH)) in which the concentrations of spin traps and reductants were varied.

### Spin trapping by DMPO

The appearance of the EPR spectrum of DMPO-OH adducts is depicted in Figure 1A. The time evaluation of the DMPO-OH adducts EPR intensity at different DMPO concentrations is represented in Figure 1B. Further incubation resulted in increasing intensity of the DMPO-OH adduct spectrum, and a prominent signal was detected at 180 minutes. A noisy spectrum was obtained in sample solutions of EPFRs (50  $\mu\text{g/ml}$ ) and DMPO (150mM) in PBS at 2 minutes of incubation. The 4 lines marked with red asterisks at 2 min incubation correspond to the DMPO-OH adduct ( $hfsc \alpha_N = \alpha_H = 14.95$  G, literature data  $\alpha_N = \alpha_H = 14.90$  G<sup>17, 27</sup>). The other 6 lines are characteristic of a carbon centered species reported in literature and identified as aminoxyl radical formed from the hydroxylamine impurity in DMPO, or formed immediately as high purity DMPO is transferred in an oxygen rich environment<sup>28, 29</sup>. The EPR intensity of this impurity decreases slowly with time and does not interfere with the measurements of DMPO-OH adduct generation. To provide sufficient EPR intensity for convenient analysis, but avoid potential secondary reactions (Decomposition by light, oxidation by dissolved oxygen, reducing/oxidation, dimerization etc<sup>16</sup>) which may occur at high DMPO concentrations, a final DMPO solution concentration of 150 mM was used in all further studies.

The results of non-aeration/aeration on both non-EPFR (control) and EPFR particles solutions are presented in Figures 2 A and B. The difference in the DMPO-OH adduct spectral intensity for the sample and control solutions (calculated from the second line at low magnetic field of their respective 4 line spectra) increased with time, most notably at incubation times  $> 150$  min. This difference was larger and occurred at earlier times for the aerated solution. The difference in the non-aerated solution was only  $\sim 50\%$  at 1055 min for the non-aerated solution but was  $\sim 100\%$  for the aerated solution at only 220 min. These results confirm involvement of  $\text{O}_2$  in the redox cycle generating  $\cdot\text{OH}$ , and all further experiments were performed with aerated samples.

### Dependence of DMPO-OH adduct generation on EPFR concentration

Figure 3A depicts three sets of experimental data for the sample solutions of EPFR-containing particles (50  $\mu\text{g/ml}$ ) and DMPO (150 mM) in PBS (total 200 $\mu\text{L}$ ) with different initial concentrations of EPFRs (spins/gram). The initial rate of hydroxyl radical generation increased proportionally to the EPFR concentration when it was doubled from  $5.56 \times 10^{16}$  spins/gram and  $1.29 \times 10^{17}$  spins/gram. When the EPFR concentration was again approximately doubled to  $2.32 \times 10^{17}$  spins/gram, there was no increase in the DMPO-OH adduct concentration and the concentration actually decreased at longer incubation times. This is probably due to radical-radical recombination at high EPFR concentrations.

The dependence of DMPO-OH adduct concentration on particle concentration in solution (mg of particle/ml of solution) is depicted in Figure 3B. The intensity of DMPO-OH adduct signal exhibited a maximum at a particle concentration of 0.25 mg/ml for concentrations ranging from 0.05 to 1.0 mg/ml. For concentrations  $> 0.25$  mg/mL, the DMPO-OH concentration decreased, again, probably due to radical-radical annihilation reactions at higher concentrations. Consequently, very dilute suspensions of 50  $\mu\text{g/mL}$  were used in all subsequent experiments.

### Dependence of DMPO-OH adduct generation on EPFR aging

To determine the lifetimes of EPFRs in aqueous solution and their viability for hydroxyl radical generation, a time evaluation of DMPO-OH spectral intensity was performed for particles allowed to age in room air over a period of a week (cf. Figure 4). A stock solution of EPFR-containing particles (50 µg/ml) and DMPO (150mM) in PBS (total 200µL) was prepared, and fresh sample solutions were subjected to the spin trapping procedure each day. A marked increase in the DMPO-OH adduct intensity was detected on the third day. Concomitantly, the concentration of the EPFRs on the catalyst surface was measured. For the latter, the solutions were subjected to agitation, decanting, and vacuum drying before the residue solid powder was subjected EPR examination. On the first day, the sample exhibited a singlet EPR spectrum ( $g=2.0042$ ,  $\Delta H_{p-p} = 6.5$  G) which matched well with the initial spectra before aging. This signal remained strong through the third day, before decaying slowly to barely detectable quantities by the seventh day. This coincided with the maximum in hydroxyl radical generation observed on day three. Thus, the observed hydroxyl radical formation is thought to be mediated, rather than catalyzed, and EPFRs are consumed in the mediated process. However, as proposed in Scheme 1, a biological reducing equivalent is necessary to complete the truly catalytic hydroxyl radical generation cycle.

### Dependence of DMPO-OH adduct generation on biological reducing equivalents

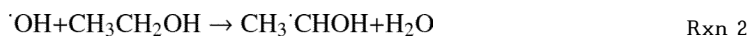
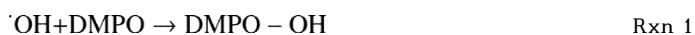
The generation of hydroxyl radical in biological systems is usually enhanced by the presence of H-donors, e.g. NADPH and ascorbates etc.<sup>30, 31</sup>. Up to 1 mM of NADPH or ascorbic acid was added to the solution of EPFR's (50 µg/mL) and DMPO (150 mM) in PBS (cf. Supporting Information). The NADPH induced a small effect; while ascorbic acid significantly increased DMPO-OH adduct formation at its lower concentrations (100 µM). However, at higher ascorbic acid concentrations (500 µM), it acted as an effective antioxidant by formation of a characteristic doublet line of ascorbyl radicals. To avoid secondary reactions involving these reductants, their use was minimized in subsequent experiments.

### Radical Scavengers

Existence of free hydroxyl radicals in biological red-ox systems is usually confirmed using solution, radical scavengers and formation of secondary radicals<sup>32, 33</sup>. The kinetic competition between DMPO and hydroxyl radical scavengers (ethanol, DMSO, sodium formate, and sodium azide) is used to establish or rule out the presence of free hydroxyl radical. Otherwise, the hydroxyl radical may be bound, or associated with a surface or other molecular species. The effect of scavengers on radical formation were performed in the sample solutions used previously.

Inhibition of DMP-OH adduct formation was observed with addition of 10% (v/v) EtOH at 50 min incubation time (cf. Figure 5A). Thirty minutes later the intensity was decreased by 20 % ( $DI/N = 20$ ) and then slightly increased. The effect of different ethanol concentrations on inhibition of DMP-OH adduct formation is presented in Figure 5B.

Hydroxyl radicals in the presence of DMPO and ethanol can undergo the competitive reactions:



and the new radical  $\text{CH}_3\dot{\text{C}}\text{HOH}$  will be trapped by DMPO via:

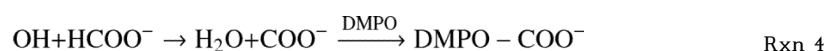


The resulting DMPO-1-hydroxyethyl adduct exhibits a characteristic 6 line spectrum, *vide infra*<sup>34, 35</sup>. If this reaction occurs, the DMPO-OH signal should decrease as the DMPO-CH(CH<sub>3</sub>)OH signal increased. This was not observed, suggesting the reaction of ethanol and hydroxyl radical did not occur.

DMSO is also a good scavenger of free hydroxyl radicals via reactions similar to Rxns. 1 and 2 for ethanol<sup>34</sup>. At low concentration (2%, v/v), DMSO was a promoter of DMPO-OH formation, while at > 10% concentration, it completely inhibited formation, (cf. Figure 6). As in case of ethanol, no concomitant formation of the DMPO-CH<sub>3</sub> adduct, 6-line EPR spectrum was detected.

In an attempt to generate observable free hydroxyl radical, 20 mM of hydrogen peroxide was added to both the EtOH- and DMSO-containing solutions<sup>36</sup>. Generation of hydroxyl radical by H<sub>2</sub>O<sub>2</sub> has been reported in the presence of Cu(II) ions and CuO micron-sized catalyst particles<sup>36, 37</sup>. The Cu(I), present in our EPFR-containing particles (Scheme 1), should also react with the peroxide via Fenton-type reactions to produce hydroxyl radical. The results are summarized in Figure 7 for the EPR spectra of DMPO-OH adduct (blue line). The EPR spectra of DMPO-CH(CH<sub>3</sub>)-OH adduct (red line), marked by asterisks, was derived from the solution of EPFRs, DMPO, and ethanol (30 %,v/v) + H<sub>2</sub>O<sub>2</sub> (20 mM). The observed EPR spectral parameters (hfsc:  $\alpha_{\text{N}} = 15.1 \text{ G}$ ,  $\alpha_{\text{H}}^{\beta} = 23.1 \text{ G}$ ) agreed well with the literature values ( $\alpha_{\text{N}} = 15.8 \text{ G}$ ,  $\alpha_{\text{H}}^{\beta} = 22.8 \text{ G}$ <sup>34</sup>). The EPR spectra of DMPO-CH<sub>3</sub> adduct (black line), marked by asterisks, was generated from a solution of EPFRs, DMPO and DMSO (10 %,v/v) + H<sub>2</sub>O<sub>2</sub> (20 mM). The spectral parameters (hfsc of  $\alpha_{\text{N}} = 16.8 \text{ G}$ ,  $\alpha_{\text{H}}^{\beta} = 23.8 \text{ G}$ ) also agreed well with the literature ( $\alpha_{\text{N}} = 16.4 \text{ G}$ ,  $\alpha_{\text{H}}^{\beta} = 23.4 \text{ G}$ <sup>34</sup>). These results suggest free hydroxyl radicals generated by the EPFR particle systems should have been detected in the previously tested solutions if they were present.

Formate and sodium azide were also used in an attempt to scavenge free hydroxyl radical via the reactions:



Neither the characteristic 6-line spectrum of DMPO-COO<sup>-</sup> nor the 12-line spectrum of DMPO-N<sub>3</sub> was detected<sup>35</sup>. These lines were generated only following addition of H<sub>2</sub>O<sub>2</sub> (20 mM in solution) as a source of free hydroxyl radicals (data not shown).

### Free versus bound hydroxyl radical

The DMPO spin trapping results indicate hydroxyl radical is being generated. However, the failure of scavenging hydroxyl radicals to form secondary radicals in solution, suggests they are not truly free hydroxyl radicals. Several observations support this contention.

1. The control solutions, containing Cu(II)O/siica, generate free hydroxyl radical, as evidenced by the scavenger results (not shown), only when hydrogen peroxide is added. The detection of DMPO-OH adducts without the addition of hydrogen peroxide is likely due to the Cu(II) or Fe(III) impurity, catalyzed nucleophilic addition of water to DMPO<sup>16, 17, 38</sup>. This has been proposed in the literature, but the issue is by no means settled<sup>39-42</sup>. The non-radical nucleophilic reaction of water has been proposed to be a significant pathway to the formation of DMPO-OH radical adducts, even during a Fenton reaction<sup>40, 41</sup>, i.e. 80-90% of the total DMPO-OH in <sup>17</sup>O-enriched water was due to iron-dependent nucleophilic addition of water<sup>41</sup>. However, the same authors also discuss a water-independent mechanism of DMPO-OH formation<sup>41</sup>, and how Fe or Cu ion-induced nucleophilic addition of water to DMPO may be significantly suppressed in experiments performed in most common buffers<sup>40</sup>.

2. The observed DMPO-OH adducts may form due to a secondary mechanism not involving hydroxyl radical trapping<sup>43</sup>. DMPO-OH adduct formation has been proposed to be the result of conversion of DMPO – superoxide adduct (DMPO-OOH)<sup>34, 43-45</sup>. However, only 3% of DMPO-OOH adduct has been reported to be converted into DMPO-OH<sup>34</sup>, and the concentration of DMPO-OH adduct may be affected only when there is a high concentration of superoxide radicals<sup>46</sup>. Other researchers have reported that this conversion does not occur<sup>47</sup>.

Another secondary mechanism might be oxidation of DMPO through its cation radical, by addition of water (and elimination of a proton) with ultimate formation of DMPO-OH adduct<sup>48</sup>. This, as well as all other possible conversions of DMPO in aqueous solution (oxidation by dissolved oxygen, dimerization, reduction/oxidation, etc.), may occur and every specific case must be considered. The differences we have observed in accumulation of DMPO-OH adducts between the control and sample solutions (cf. Figure 2) and the direct dependency of the intensity of DMPO-OH adducts on EPFR concentration per gram of particle (cf. Figure 3A) are explained by the activity of EPFRs. Other potential explanations appear to apply to both the samples and controls.

3. Scheme 1 depicts how hydroxyl radicals can be generated by a surface-catalyzed, redox cycle. Our results indicate hydroxyl radical is produced and forms adducts with DMPO, but the concentration of free hydroxyl radical in solution is too low to be scavenged to form secondary radicals or the rate of reaction with the secondary radicals with DMPO is too slow to be easily detectable. The rate coefficient for reaction of hydroxyl radicals with organics has been reported to be  $(2.1-5.7) \times 10^9 \text{ M}^{-1} \cdot \text{s}^{-1}$  for reaction 1 and  $1.8 \times 10^9 \text{ M}^{-1} \cdot \text{s}^{-1}$  for reaction 2<sup>49</sup>, while the reaction coefficient for secondary  $\cdot\text{CH}(\text{CH}_3)\text{OH}$  radicals, formed by the ethanol scavenger has been reported to be two orders of magnitude slower, viz.  $4.1 \times 10^7 \text{ M}^{-1} \cdot \text{s}^{-1}$  for reaction 3<sup>50</sup>. Using these rate constants it can be easily established that reaction 3 may compete with reaction 1 at a ratio of concentration of secondary to hydroxyl radicals of  $\sim 100$ . Thus, it appears the secondary radicals cannot compete with hydroxyl radicals to be trapped by DMPO unless the concentration of  $\cdot\text{CH}(\text{CH}_3)\text{OH}$  is much greater than hydroxyl radical.

To determine the minimum concentration of hydroxyl radicals that could be effectively detected using DMPO, additional experiments using hydrogen peroxide to generate hydroxyl radical were performed. The ability of sample solutions to generate DMPO-OH adducts at hydrogen peroxide concentrations of 1.5, 0.3, 0.06, and 0.006 mM was determined. The minimum concentration of hydrogen peroxide necessary to generate more DMPO-OH adduct than the EPFR-containing particles during the first 100 minutes is between 0.006 and 0.06 mM (cf. Figure 8 A, blue, pink and black lines). The question is then at what minimum concentration of hydrogen peroxide, assuming the hydroxyl radicals

are free in solution, secondary  $\cdot\text{CH}(\text{CH}_3)\text{OH}$  might be generated in detectable quantities. Thus, the previous experiments were repeated in the presence of a large excess (1.7 M) of ethanol scavenger. The characteristic 6 lines of the DMPO- $\text{CH}(\text{CH}_3)\text{OH}$  adduct<sup>34, 35</sup> were barely detectable and were only clearly identifiable when the hydrogen peroxide concentration was increased to 0.25mM and above (cf. Figure 8 B). At < 0.25 mM hydrogen peroxide, the scavenging efficiency of ethanol is not high enough to form detectable secondary radicals. Thus, a more effective spin trap for secondary radicals is needed with a scavenging rate coefficient  $>4.1 \times 10^7 \text{ M}^{-1} \cdot \text{s}^{-1}$ <sup>50</sup>, or a more sensitive EPR method, which can detect less than  $10^{-6} \text{ M}$  in solutions<sup>51, 52</sup>, must be employed. For instance, the detection limit of particle-generated hydroxyl radicals can be quantified at a concentration of only 50 nM by a fluorescence-based technique using 3'-(p-aminophenyl) fluorescein (APF)<sup>53</sup>. However, this technique may not have sufficient specificity<sup>44, 45, 53, 54</sup>. New EPR spin trapping techniques employing heteroaryl nitrones may be useful since they have been reported to be highly soluble in water, are less sensitive to nucleophilic attack, have long half-lives of the spin adducts, and exhibit high selectivity<sup>55</sup>.

Based on all these experiments, we believe hydroxyl radicals are generated by the surface-mediated cycle in Scheme 1, with the resulting hydroxyl radicals remaining primarily on the surface such that they cannot be readily scavenged to form secondary organic radicals. This hypothesis is not without experimental or theoretical precedence<sup>56-62, 63</sup>. For example, oxidizing metal sites have been proposed to form and trap hydroxyl radicals with reactivities similar (but distinguishable) to those of free hydroxyl radical<sup>64, 65</sup>. The surface bound hydroxyl radicals have even been suggested of being capable of oxidizing of substrates which are oxidized by free hydroxyl radical<sup>56</sup>. In our theory, the combination of the surface-bound hydroxyl radical and the reduced metal in the immediate vicinity are responsible for this enhanced activity of the particles.

## Supplementary Material

Refer to Web version on PubMed Central for supplementary material.

## Acknowledgments

The authors gratefully acknowledge the partial support of this research from NIEHS as part of the LSU Superfund Center under Superfund Research and Training Program grant P42ES13648.

## Literature Cited

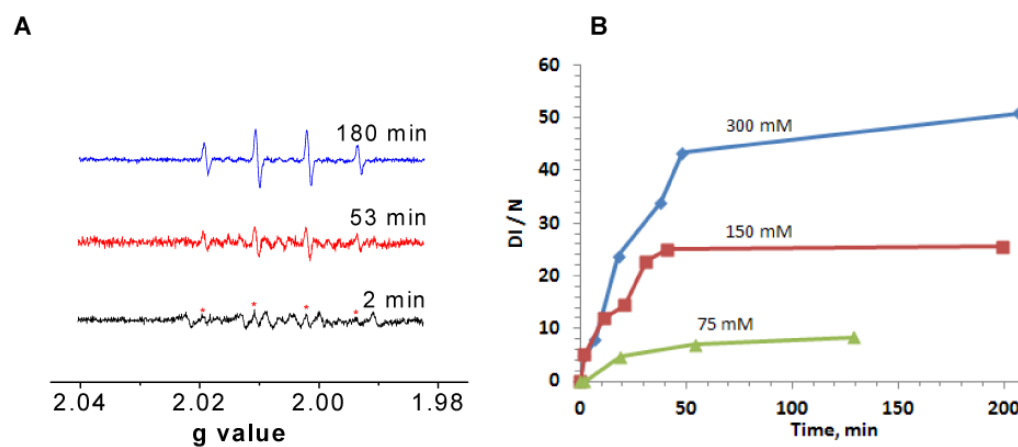
1. Dellinger B, Pryor WA, Ceuto R, Squadrito GL, Hedge V, Deutsch WA. Role of free radicals in the toxicity of airborne fine particulate matter. *Chem Res Toxicol*. 2001; 14:1371–1377. [PubMed: 11599928]
2. Dellinger B, Lomnicki S, Khachatryan L, Maskos Z, Hall R, Adoukpe J, McFerrin C, Truong H. Formation and stabilization of persistent free radicals. *Proceedings of the Combustion Institute*. 2007; 31:521–528.
3. Lomnicki S, Truong H, Vejerano E, Dellinger B. Copper oxide-based model of persistent free radical formation on combustion-derived particulate matter. *Environ Sci & Technol*. 2008; 42(13): 4982–4988. [PubMed: 18678037]
4. Valavanidis A, Iopoulou N, Gotsis G, Fiotakis K. Persistent free radicals, heavy metals and PAHs generated in particulate soot emissions and residue ash from controlled combustion of common types of plastic. *J Hazard Mater*. 2008; 156(1-3):277–284. [PubMed: 18249066]
5. McFerrin CA, Hall RW, Dellinger B. Ab Initio study of the formation and degradation reactions of chlorinated phenols. *J Molecular Structure*. 2009; 902(1-3):5–14.
6. Dellinger B, Pryor WA, Cueto R, Squadrito GL, Deutsch WA. The role of combustion-generated radicals in the toxicity of PM2.5. *Proceedings of the Combustion Institute*. 2000; 28:2675–2681.



7. Cormier SA, Lomnicki S, Backes W, Dellinger B. Origin and health impacts of emissions of toxic by-products and fine particles from combustion and thermal treatment of hazardous wastes and materials. *Environ Health Perspect.* 2006; 114:810–817. [PubMed: 16759977]
8. Khachatryan L, Vejerano E, Lomnicki S, Dellinger B. Environmentally Persistent Free Radicals (EPFRs) *In Vitro* Experiments. 1. Generation of Reactive Oxygen Species (ROS) in Aqueous Solutions. *Environ Sci & Technol.* 2011 in press.
9. Halliwell B, Gutteridge JMC. Free Radicals and Metal Ions in Human Disease in *Methods in Enzymology.* 1990; 186:1–85. [PubMed: 2172697]
10. Fridovich I. Superoxide Radical - an Endogenous Toxicant. *Annual Review of Pharmacology and Toxicology.* 1983; 23:239–257.
11. Halliwell B. Oxidative Stress and Disease. 2001; 7:1–16.
12. Zweier JL, Talukder MAH. The role of oxidants and free radicals in reperfusion injury. *Cardiovascular Research.* 2006; 70(2):181–190. [PubMed: 16580655]
13. Forshult S, Lagercrantz C. Use of Nitroso Compounds as Scavengers for Study of Short-Lived Free Radicals in Organic Reactions. *Acta Chemica Scandinavica.* 1969; 23(2):522–523.
14. Janzen EG, Blackburn BJ. Detection and Identification of Short-Lived Free Radicals by an Electron Spin Resonance Trapping Technique. *J Am Chem Soc J1 - JACS.* 1968; 90(21):5909–5910.
15. Harbour JR, Chow V, Bolton JR. Electron-Spin Resonance Study of Spin Adducts of OH and HO<sub>2</sub> Radicals with Nitrones in Ultraviolet Photolysis of Aqueous Hydrogen-Peroxide Solutions. *Canadian Journal of Chemistry-Revue Canadienne De Chimie.* 1974; 52(20):3549–3553.
16. Finkelstein E, Rosen GM, Rauckman EJ. Spin Trapping of Superoxide and Hydroxyl Radical - Practical Aspects. *Arch Biochem Biophys.* 1980; 200(1):1–16. [PubMed: 6244786]
17. Makino K, Hagiwara T, Murakami A. Fundamental-Aspects of Spin Trapping with Dmpo. *Radiation Physics and Chemistry.* 1991; 37(5-6):657–665.
18. Truong, H. Dissertation for PhD degree. LSU, LA: 2007. Copper (II) oxide mediated formation and stabilization of combustion generated persistent free radicals.
19. Truong H, Lomnicki S, Dellinger B. Potential for Misidentification of Environmentally Persistent Free Radicals as Molecular Pollutants in Particulate Matter. *Environmental Science & Technology.* 2010; 44(6):1933–1939. [PubMed: 20155937]
20. Eaton, GR.; Eaton, SS.; Barr, DP.; Weber, RT. *Quantitative EPR.* SpringerWien; NewYork (Germany): 2010. p. 185
21. Nakagawa K. Is quartz flat cell useful for the detection of superoxide radicals? *J Act Oxyg Free Rad.* 1994; 5:81–85.
22. Fubini B, Mollo L, Giamello E. Free radical generation at the solid/liquid interface in iron containing minerals. *Free Rad Res.* 1995; 23(6):593–614.
23. Tomita M, Okuyama T, Watanabe S, Watanabe H. Quantitation of the Hydroxyl Radical Adducts of Salicylic-Acid by Micellar Electrokinetic Capillary Chromatography -Oxidizing Species Formed by a Fenton Reaction. *Archives of Toxicology.* 1994; 68(7):428–433. [PubMed: 7979959]
24. Yamazaki I, Piette LH. Epr Spin-Trapping Study on the Oxidizing Species Formed in the Reaction of the Ferrous Ion with Hydrogen-Peroxide. *J Am Chem Soc J1 - JACS.* 1991; 113(20):7588–7593.
25. Zhu BZ, Har-El R, Kitrossky N, Chevion M. New modes of action of desferrioxamine: scavenging of semiquinone radical and stimulation of hydrolysis of tetrachlorohydroquinone. *Free Radical Biology and Medicine.* 1998; 24(5):880–880.
26. Finkelstein E, Rosen GM, Rauckman EJ. Spin Trapping - Kinetics of the Reaction of Superoxide and Hydroxyl Radicals with Nitrones. *J Am Chem Soc J1 - JACS.* 1980; 102(15):4994–4999.
27. Harbour JR, Bolton JR. Involvement of Hydroxyl Radical in Destructive Photo-Oxidation of Chlorophylls *In Vivo* and *In Vitro*. *Photochem Photobiol.* 1978; 28(2):231–234.
28. Buettner GR, Oberley LW. Considerations in Spin Trapping of Superoxide and Hydroxyl Radical in Aqueous Systems Using 5,5-Dimethyl-1-Pyrroline-1-Oxide. *Biochemical and Biophysical Research Communications.* 1978; 83(1):69–74. [PubMed: 212052]

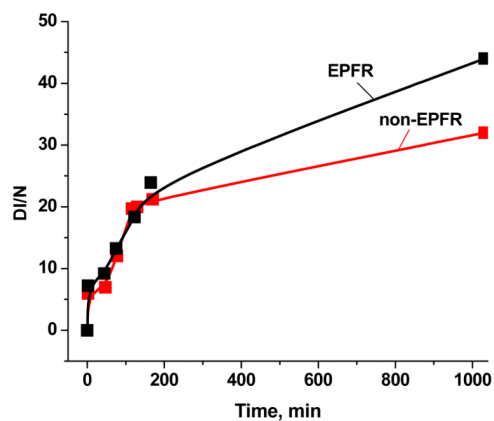
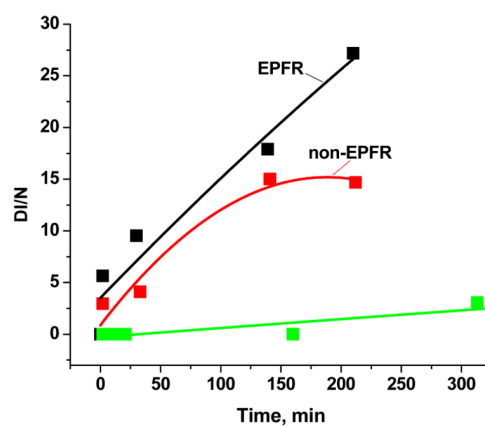
29. Makino K, Imaishi H, Morinishi S, Hagiwara T, Takeuchi T, Murakami A, Nishi M. An Artifact in the ESR-Spectrum Obtained by Spin Trapping with Dmpo. *Free Radical Research Communications*. 1989; 6(1):19–28. [PubMed: 2542138]
30. Alaghmand M, Blough NV. Source-dependent variation in hydroxyl radical production by airborne particulate matter. *Environmental Science & Technology*. 2007; 41(7):2364–2370. [PubMed: 17438788]
31. Briede JJ, De Kok TMCM, Hogervorst JGF, Moonen EJC, Den Camp CLBO, Kleinjans JCS. Development and application of an electron spin resonance spectrometry method for the determination of oxygen free radical formation by particulate matter. *Environmental Science & Technology*. 2005; 39(21):8420–8426. [PubMed: 16294882]
32. Yim MB, Chock PB, Stadtman ER. Copper, Zinc Superoxide-Dismutase Catalyzes Hydroxyl Radical Production from Hydrogen-Peroxide. *Proceedings of the National Academy of Sciences of the United States of America*. 1990; 87(13):5006–5010. [PubMed: 2164216]
33. Buettner, GR.; Mason, RP. Critical reviews of oxidative stress and aging: Advances in basic science, diagnostics and intervention Chapter 2. Cutler, RG.; Rodrigues, H., editors. 2003. p. 27-38.
34. Finkelstein E, Rosen GM, Rauckman EJ. Production of Hydroxyl Radical by Decomposition of Superoxide Spin-Trapped Adducts. *Molecular Pharmacology*. 1982; 21(2):262–265. [PubMed: 6285165]
35. Zhu BZ, Zhao HT, Kalyanaraman B, Frei B. Metal-independent production of hydroxyl radicals by halogenated quinones and hydrogen peroxide: An ESR spin trapping study. *Free Radical Biology and Medicine*. 2002; 32(5):465–473. [PubMed: 11864786]
36. Kim JK, Metcalfe IS. Investigation of the generation of hydroxyl radicals and their oxidative role in the presence of heterogeneous copper catalysts. *Chemosphere*. 2007; 69(5):689–696. [PubMed: 17604820]
37. Ozawa T, Hanaki A. The 1st ESR Spin-Trapping Evidence for the Formation of Hydroxyl Radical from the Reaction of Copper(II) Complex with Hydrogen-Peroxide in Aqueous-Solution. *Journal of the Chemical Society-Chemical Communications*. 1991; (5):330–332.
38. Burkitt MJ, Tsang SY, Tam SC, Bremner I. Generation of 5,5-Dimethyl-1-Pyrroline N-Oxide Hydroxyl and Scavenger Radical Adducts from Copper/H<sub>2</sub>O<sub>2</sub> Mixtures - Effects of Metal-Ion Chelation and the Search for High-Valent Metal-Oxygen Intermediates. *Arch Biochem Biophys*. 1995; 323(1):63–70. [PubMed: 7487075]
39. Makino K, Hagiwara T, Hagi A, Nishi M, Murakami A. Cautionary Note for Dmpo Spin Trapping in the Presence of Iron-Ion. *Biochemical and Biophysical Research Communications*. 1990; 172(3):1073–1080. [PubMed: 2173913]
40. Hanna PM, Chamulitrat W, Mason RP. When Are Metal Ion-Dependent Hydroxyl and Alkoxy Radical Adducts of 5,5-Dimethyl-1-Pyrroline N-Oxide Artifacts. *Arch Biochem Biophys*. 1992; 296(2):640–644. [PubMed: 1321591]
41. Chamulitrat W, Iwahashi H, Kelman DJ, Mason RP. Evidence against the 1-2-2-1 Quartet Dmpo Spectrum as the Radical Adduct of the Lipid Alkoxy Radical. *Arch Biochem Biophys*. 1992; 296(2):645–649. [PubMed: 1321592]
42. Alegria AE, Ferrer A, Sepulveda E. Photochemistry of water-soluble quinones. Production of a water-derived spin adduct. *Photochem Photobiol*. 1997; 66(4):436–442. [PubMed: 9337614]
43. Finkelstein E, Rosen GM, Rauckman EJ, Paxton J. Spin Trapping of Superoxide. *Molecular Pharmacology*. 1979; 16(2):676–685. [PubMed: 229403]
44. Roubaud V, Sankarapandi S, Kuppusamy P, Tordo P, Zweier JL. Quantitative measurement of superoxide generation using the spin trap 5-(diethoxyphosphoryl)-5-methyl-1-pyrroline-N-oxide. *Analytical Biochemistry*. 1997; 247(2):404–411. [PubMed: 9177705]
45. Bacic G, Spasojevic I, Secerov B, Mojovic M. Spin-trapping of oxygen free radicals in chemical and biological systems: New traps, radicals and possibilities. *Spectrochimica Acta Part a-Molecular and Biomolecular Spectroscopy*. 2008; 69(5):1354–1366.
46. Pou S, Cohen MS, Britigan BE, Rosen GM. Spin-Trapping and Human-Neutrophils - Limits of Detection of Hydroxyl Radical. *Journal of Biological Chemistry*. 1989; 264(21):12299–12302. [PubMed: 2545706]

47. Shi HL, Timmins G, Monske M, Burdick A, Kalyanaraman B, Liu Y, Clement JL, Burchiel S, Liu KJ. Evaluation of spin trapping agents and trapping conditions for detection of cell-generated reactive oxygen species. *Arch Biochem Biophys*. 2005; 437(1):59–68. [PubMed: 15820217]
48. Eberson L. *Advances in physical organic chemistry*. 1998; 31:91–141.
49. Dorfman LM, Adams GE. Reactivity of the hydroxyl radical in aqueous solutions. *Nat Stand ref Data Ser Nat Bur Stand*. 1973:46. NSRDS-NBS.
50. Brustolon, M.; Giamello, E. *Electron Paramagnetic Resonance A practitioner's toolkit*. Wiley; New Jersey: 2009.
51. Buettner GR. Spin Trapping - Electron-Spin-Resonance Parameters of Spin Adducts. *Free Radical Biology and Medicine*. 1987; 3(4):259–303. [PubMed: 2826304]
52. Harbour JR, Hair ML. Transient Radicals in Heterogeneous Systems - Detection by Spin Trapping. *Advances in Colloid and Interface Science*. 1986; 24(2-3):103–141. [PubMed: 2849955]
53. Cohn CA, Pedigo CE, Hylton SN, Simon SR, Schoonen MAA. Evaluating the use of 3'-(p-Aminophenyl) fluorescein for determining the formation of highly reactive oxygen species in particle suspensions. *Geochemical Transactions*. 2009; 10(8)10.1186/1467-4866-10-8
54. Li BB, Gutierrez PL, Blough NV. Trace determination of hydroxyl radical in biological systems. *Anal Chem*. 1997; 69(21):4295–4302. [PubMed: 9360488]
55. Barriga G, Olea-Azar C, Norambuena E, Castro A, Porcal W, Gerpe A, Gonzalez M, Cerecetto H. New heteroaryl nitrones with spin trap properties: Identification of a 4-furoxanyl derivative with excellent properties to be used in biological systems. *Bioorganic & Medicinal Chemistry*. 2010; 18(2):795–802. [PubMed: 20031416]
56. Tojo S, Tachikawa T, Fujitsuka M, Majima T. Oxidation processes of aromatic sulfides by hydroxyl radicals in colloidal solution of TiO<sub>2</sub> during pulse radiolysis. *Chem Phys Lett*. 2004; 384(4-6):312–316.
57. Hodgson EK, Fridovich I. Interaction of Bovine Erythrocyte Superoxide-Dismutase with Hydrogen-Peroxide - Inactivation of Enzyme. *Biochemistry*. 1975; 14(24):5294–5299. [PubMed: 49]
58. Hodgson EK, Fridovich I. Interaction of Bovine Erythrocyte Superoxide-Dismutase with Hydrogen-Peroxide - Chemiluminescence and Peroxidation. *Biochemistry*. 1975; 14(24):5299–5303. [PubMed: 172122]
59. Lawless D, Serpone N, Meisel D. Role of OH Radicals and Trapped Holes in Photocatalysis - a Pulse-Radiolysis Study. *J Phys Chem*. 1991; 95(13):5166–5170.
60. Donaldson K, Brown DM, Mitchell C, Dineva M, Beswick PH, Gilmour P, MacNee W. Free radical activity of PM10: Iron-mediated generation of hydroxyl radicals. *Environ Health Perspect*. 1997; 105:1285–1289. [PubMed: 9400739]
61. Venkatachari P, Hopke PK, Brune WH, Ren XR, Leshner R, Mao JQ, Mitchel M. Characterization of wintertime reactive oxygen species concentrations in Flushing, New York. *Aerosol Science and Technology*. 2007; 41(2):97–111.
62. Chen X, Hopke PK, Carter WPL. Secondary Organic Aerosol from Ozonolysis of Biogenic Volatile Organic Compounds: Chamber Studies of Particle and Reactive Oxygen Species Formation. *Environmental Science & Technology*. 2011; 45(1):276–282. [PubMed: 21121662]
63. Narayanasamy J, Kubicki JD. Mechanism of hydroxyl radical generation from a silica surface: Molecular orbital calculations. *J Phys Chem B*. 2005; 109(46):21796–21807. [PubMed: 16853831]
64. Lloyd RV, Hanna PM, Mason RP. The origin of the hydroxyl radical oxygen in the Fenton reaction. *Free Radical Biology and Medicine*. 1997; 22(5):885–888. [PubMed: 9119257]
65. Borda MJ, Elsetinow AR, Strongin DR, Schoonen MA. A mechanism for the production of hydroxyl radical at surface defect sites on pyrite. *Geochimica Et Cosmochimica Acta*. 2003; 67(5): 935–939.

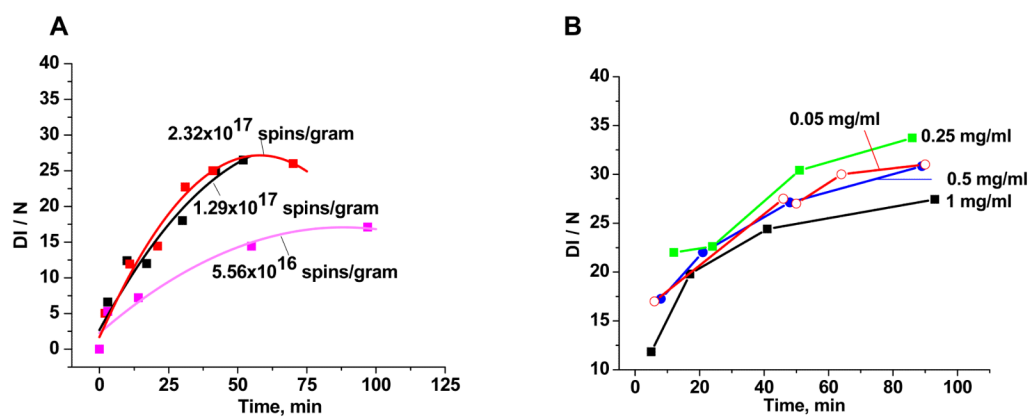


**Figure 1.**

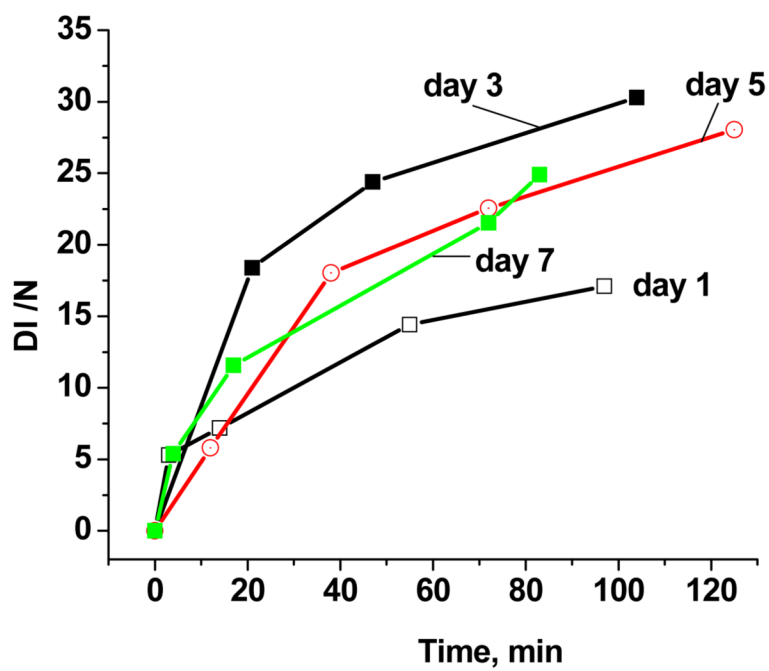
**A.** Evaluation of EPR spectra of DMPO-OH adducts as a function of incubation time for a solution of EPFRs (50  $\mu\text{g}/\text{ml}$ ), DMPO (150 mM) in PBS. **B.** Time dependence of EPR spectral intensity of DMPO-OH adducts as a function of DMPO concentration in solution.

**A. Non-aerated solution****B. Aerated solution**

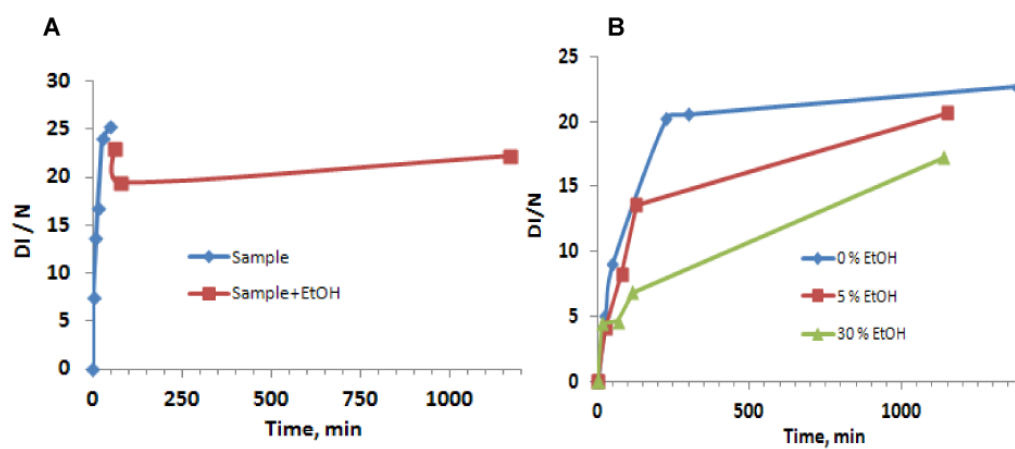
**Figure 2.** **A.** The time evolution of the EPR signal intensity of DMPO-OH for the *non-aerated* control (red) and sample (black) solutions. **B.** The time evaluation of the EPR signal intensity of DMPO-OH for the *aerated* control (red) and sample (black) solutions. The green line represents the time evaluation of the EPR signal intensity of DMPO-OH for pure DMPO (150 mM) in 200  $\mu$ L PBS solution and indicates no statistical increase in DMPO-OH concentration.



**Figure 3.** EPR spectral intensity of DMPO-OH as a function of EPFR concentration (spins/g) and incubation time. **A.** The initial EPFR concentration on the particles was parametrically varied (radicals/g of particle). **B.** The initial particle concentration in solution was varied (mg of particle/ml).



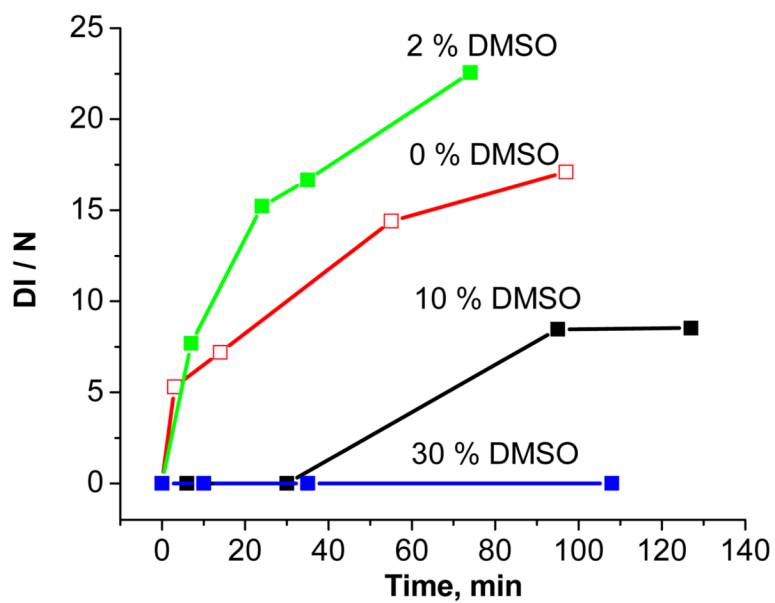
**Figure 4.** EPR spectral intensity of DMPO-OH adducts as a function of incubation time for solution allowed to age over 1 to 7 days while exposed to air.



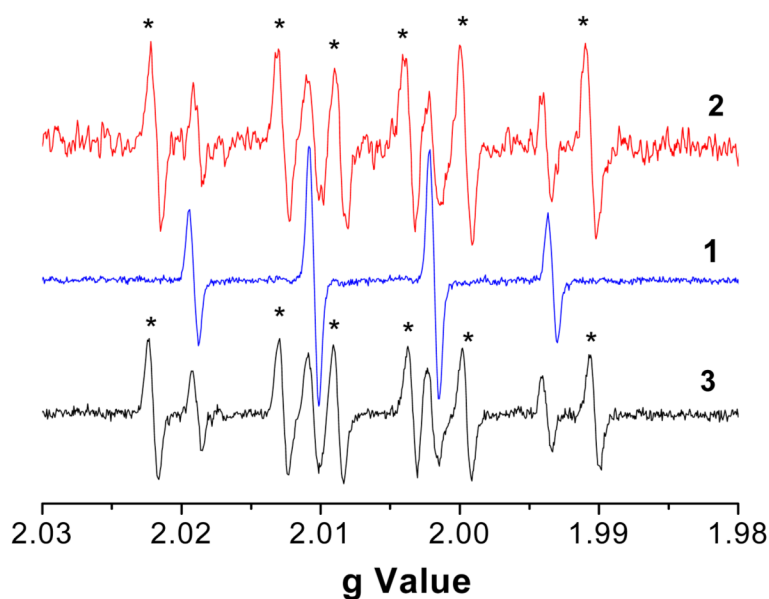
**Figure 5.**

**A.** The inhibitory effect of EtOH 10% (v/v) on DMPO-OH EPR signal intensity (DI / N) added after 50 minutes incubation for a sample solution of EPFRs (50 ug/ml) + DMPO (150 mM) + PBS. **B.** Time dependence of DMPO-OH adduct intensity as a function of ethanol concentration (percent, v/v).



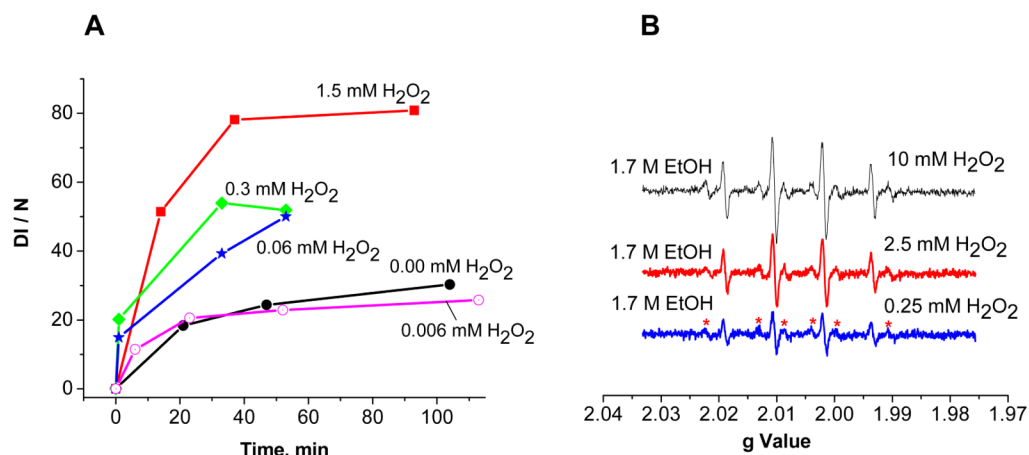


**Figure 6.** Time evaluation of DMPO-OH adduct intensity (DI/N) as a function of DMSO concentration (percent, v/v) in water solution (EPFRs (50ug/ml) and DMPO (150 mM) in PBS).



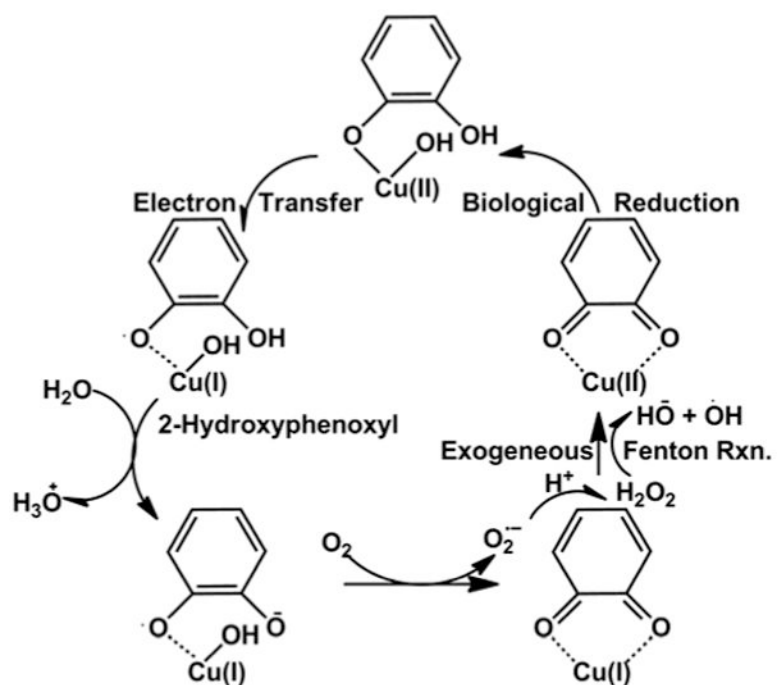
**Figure 7.**

EPR spectra of spin adducts generated in different solutions. **1.** DMPO-OH in solution of EPFRs (50  $\mu\text{g}/\text{ml}$ ) and DMPO(150 mM) in PBS +  $\text{H}_2\text{O}_2$  (20 mM). **2.** Mixture of DMPO-OH and DMPO-CH(CH<sub>3</sub>)OH in solution of EPFRs (50  $\mu\text{g}/\text{ml}$ ), DMPO (150 mM), and EtOH (30% v/v) in PBS +  $\text{H}_2\text{O}_2$  (20 mM). **3.** Mixture of DMPO-OH and DMPO-CH<sub>3</sub> in a solution of EPFRs (50  $\mu\text{g}/\text{ml}$ ), DMPO(150 mM), and DMSO (10% v/v) in PBS +  $\text{H}_2\text{O}_2$  (20 mM). The background DMPO-OH EPR signal after 5 min without addition of  $\text{H}_2\text{O}_2$  was extremely weak (data not shown).



**Figure 8.**

**A.** Time evaluation of DMPO-OH EPR spectral intensity (DI / N) as a function of hydrogen peroxide concentration in a sample solution of EPFRs (50 $\mu$ g/ml) and DMPO (150 mM) in PBS. **B.** The minimum amount of hydrogen peroxide (0.25 mM) at which hydroxyl radical is scavenged by 1.7 M ethanol to result in a detectable 6-line spectrum of DMPO-CH(CH<sub>3</sub>)OH adduct (marked with asterisks).



**Scheme 1.** Hypothesized red-ox cycle of EPFRs (**2-hydroxyphenoxyl**) originating from 2-MCP molecule adsorbed on Cu(II) domain in biological system <sup>8</sup>.